

FINAL STATE INTERACTIONS IN ω PHOTOPRODUCTION NEAR THRESHOLD

YONGSEOK OH

*Institute of Physics and Applied Physics, Yonsei University, Seoul 120-749, Korea
E-mail: yoh@phya.yonsei.ac.kr*

T.-S. H. LEE

*Physics Division, Argonne National Laboratory, Argonne, Illinois 60439, U.S.A.
E-mail: lee@theory.phy.anl.gov*

Vector meson photoproduction and electroproduction have been suggested as a tool to find or confirm the nucleon resonances. In order to extract more reliable informations on the nucleon resonances, understanding the non-resonant background is indispensable. We consider final state interactions in ω photoproduction as a background production mechanism. For the intermediate states, we consider nucleon–vector-meson and nucleon-pion channels. The role of the final state interactions is discussed in ω meson photoproduction near threshold.

1 Introduction

Vector meson production off nucleons near threshold attracts recent interests in connection with the so-called “missing resonance problem”¹. By studying various physical quantities of vector meson production one hopes to have information on the nucleon resonances especially which couple rather strongly to the vector-meson–nucleon channel. There have been recent progress to obtain such informations by studying the processes of vector meson photoproduction^{2,3,4,5}. Among light vector mesons, ω photoproduction is studied in more detail due to its simple isospin character^{3,4}.

In order to extract information on the nucleon resonances from vector meson production, it is essential to first understand the background production mechanisms⁶. As the background non-resonant production amplitudes one considers the Pomeron exchange, one-boson exchange, and the nucleon pole terms. Then the gap between the theoretical predictions on the background production and the experimental data, e.g. in total and differential cross sections, are expected to be explained by the terms including nucleon resonances. After adjusting the resonance parameters, other physical quantities, especially polarization asymmetries, are predicted to have more conclusive evidence for the nucleon resonances and it has been shown that some polarization asymmetries are really sensitive to the presence of nucleon resonances because of different helicity structure of the production amplitudes.

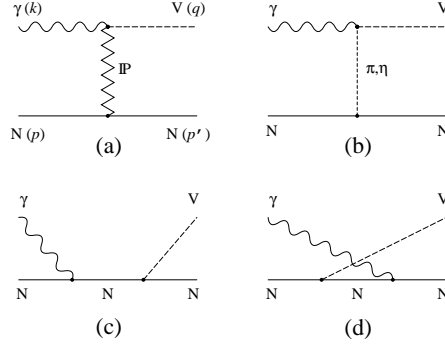


Figure 1. Non-resonant interactions for ω photoproduction at tree level. Here V stands for the ω meson.

However, in order to have more conclusive clues on the nucleon resonances, it is essential to understand the background non-resonant amplitudes in more detail. We can have lessons from the study on the non-resonant part of pion photoproduction and pion-nucleon scattering, which shows that the final state interactions are important to improve meson exchange models^{7,8}. Such dynamical studies are important not only in understanding the structure of the nucleon resonances but also for unitarity of the scattering amplitude. Therefore it is legitimate to improve the existing models by imposing unitarity condition.

Such investigations are, however, intricate and many informations are still unavailable to do a reliable model study. In this work, therefore, we study final state interactions in ω photoproduction as our first step to construct a dynamical model for vector meson photoproduction near threshold. Because of its complexity, we only consider some one-loop diagrams in this work that seem to be non-negligible in the production amplitude. In the next Section, we discuss the non-resonant amplitude at tree level and our method to compute the final state interactions for several selected intermediate channels. The preliminary numerical results are given in Sec. III with discussions.

2 Model

As the non-resonant production process for ω photoproduction at tree level, it is widely used to include the Pomeron exchange, π and η exchanges, and the nucleon pole terms as depicted in Fig. 1^{2,3,4,5}.

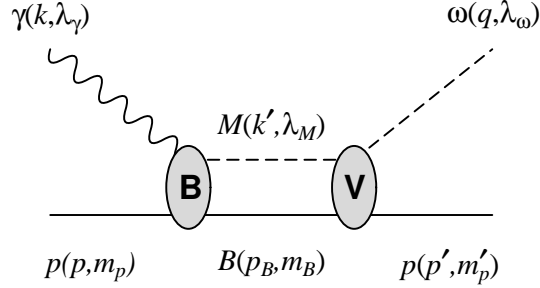


Figure 2. Diagram for final state interactions for ω photoproduction.

However, it is well-known that the amplitudes obtained at tree level such as in Fig. 1 do not satisfy unitarity. For example, the soft Pomeron model of Donnachie and Landshoff⁹ that has been used in analyzing ω photoproduction has intercept larger than 1.0 and hence violates the Froissart-Martin bound^{10,11} that is a consequence of unitarity and the partial wave expansion. Imposing the unitarity condition to the process has been emphasized in many respects^{12,13,14}. Unitarity condition is also crucial in developing dynamical models for pion photoproduction and pion-nucleon interactions^{7,8}. Therefore it would be necessary to construct a unitarized model for vector meson photoproduction near threshold to search for the “missing nucleon resonances” by, for example, solving the coupled-channel equations, which would require very complicated calculations. Before tackling to the unitarization of the amplitude directly, we first compute final state interactions by considering several selected intermediate channels. It is the purpose of this work to compute several one loop diagrams in ω photoproduction.

Following Refs.^{7,8}, what we consider is the diagram shown in Fig. 2, which defines the momenta of the interacting particles and their helicities/spins. Then the amplitude shown in Fig. 2 is written as

$$(\text{FSI})_{BM} = \int d\mathbf{k}' \frac{\langle \mathbf{q}; \lambda_\omega m'_p | V | \mathbf{k}'; \lambda_M m''_p \rangle \langle \mathbf{k}'; \lambda_M m''_p | B | \mathbf{k} \lambda_\gamma m_p \rangle}{W - E_B(\mathbf{k}') - E_M(\mathbf{k}') + i\epsilon}, \quad (1)$$

after 3-dimension reduction, where $E_{B,M}(\mathbf{k}) = \sqrt{M_{B,M}^2 + \mathbf{k}^2}$. The intermediate baryon and meson masses are denoted by M_B and M_M , respectively, and λ (m) is the helicity (spin) of the particle. Three-dimensional reduction of the full amplitude is not unique¹⁵ and we follow Refs.^{7,8} to obtain Eq. (1). It can be further decomposed into the principal integration part and the

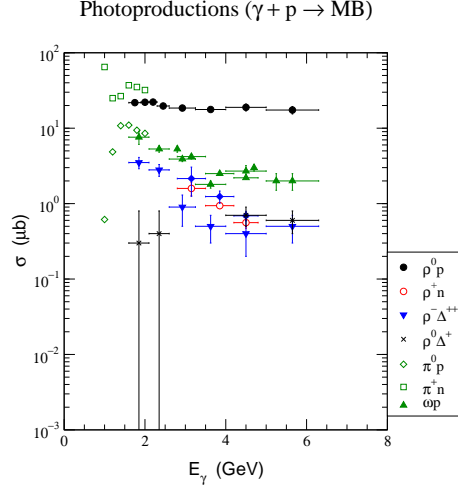


Figure 3. Collected data for the total cross sections for meson photoproduction. The data are from Ref. ¹⁶. The cross sections for $\pi^0 p$ and $\pi^+ n$ photoproductions are from Ref. ¹⁷ based on the SAID program.

delta function part as

$$\begin{aligned}
 (\text{FSI}) = \mathcal{P} \int dk' k'^2 \frac{V(q, k'; W) \mathcal{B}(k', k)}{W - E_B(k') - E_M(k')} \\
 - i \rho_{BM}(k_t) V(q, k_t; W) \mathcal{B}(k_t, k) \theta(W - M_B - M_M), \quad (2)
 \end{aligned}$$

where

$$\rho_{BM}(k) = \frac{\pi k E_B(k) E_M(k)}{[E_B(k) + E_M(k)]}, \quad (3)$$

and $\theta(x)$ is the step function ($\theta(x) = 1$ for $x > 0$ and 0 otherwise). The delta function part, which contains $\theta(x)$, arises when the intermediate particles are their on mass shell and hence the intermediate state on-shell momentum k_t is defined by

$$W = E_B(k_t) + E_M(k_t). \quad (4)$$

The intermediate states contain various baryon-meson states allowed by symmetries and quantum numbers. Therefore, we start first by selecting the intermediate states that are expected to be rather important. For this purpose, we collect some experimental informations on the cross sections of various meson photoproduction and the available experimental data are shown

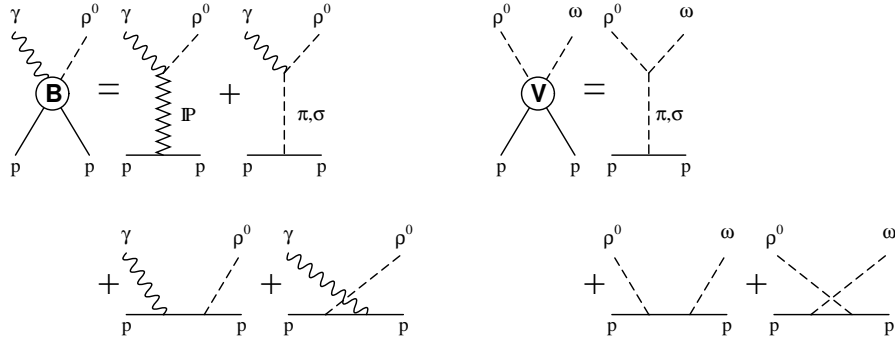


Figure 4. ω photoproduction with intermediate ρ^0 - p state.

in Fig. 3. One can see that the cross sections of π and ρ photoproductions are considerably larger than the other reactions. Based on this observation, we consider the intermediate π^+n , π^0p , and ρ^0p states.

We first consider the intermediate ρ^0p state, which is depicted in Fig. 4. Through the studies on ρ photoproduction, we have learned that the σ meson exchange is important at low energies^{6,18}. Thus our amplitude for $\gamma p \rightarrow \rho^0 p$ contains the Pomeron exchange, π exchange, σ exchange and nucleon pole terms as given in Ref.⁶. The amplitude for $\rho^0 p \rightarrow \omega p$ is closely related to the ω photoproduction amplitude at tree level that is given in Fig. 1 via vector meson dominance. In addition to vector meson dominance, what we need is the $\omega\rho\pi$ interaction Lagrangian, which reads

$$\mathcal{L}_{\omega\rho\pi} = \frac{g_{\omega\rho\pi}}{2} \varepsilon^{\mu\nu\alpha\beta} \partial_\mu \omega_\nu \text{Tr} (\partial_\alpha \rho_\beta \pi), \quad (5)$$

where $\varepsilon^{0123} = +1$, $\pi = \boldsymbol{\pi} \cdot \boldsymbol{\tau}$, $\rho = \boldsymbol{\rho} \cdot \boldsymbol{\tau}$. The coupling constant $g_{\omega\rho\pi}$ was estimated by vector meson dominance, massive Yang-Mills approach, and hidden gauge symmetry approach, etc^{19,20,21,22,23} and the estimates are within $10 \sim 15 \text{ GeV}^{-1}$. In our study, we use

$$g_{\omega\rho\pi} = 12.9 \text{ GeV}^{-1}, \quad (6)$$

where its sign is fixed by SU(3) flavor symmetry. Therefore our amplitude for $\rho^0 p \rightarrow \omega p$ contains the pion exchange and the nucleon pole terms.

For intermediate pion-nucleon channel, we need to know the non-resonant part of pion photoproduction. But the most meson-exchange models are constructed to focus on the lower energy region, so its direct extension to our energy region, $W \simeq 2 \text{ GeV}$, is quite questionable. Because of this reason,

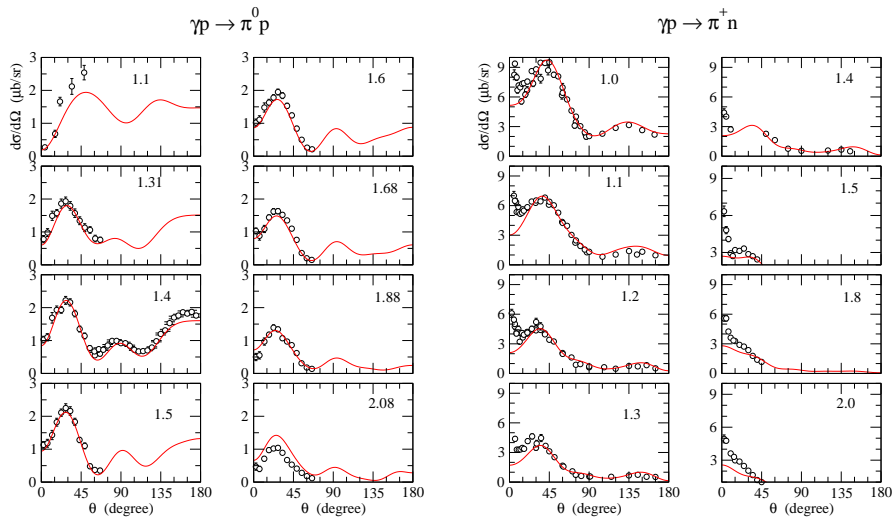


Figure 5. Differential cross sections for $\gamma p \rightarrow \pi^0 p$ and $\gamma p \rightarrow \pi^+ n$. The numbers in figures represent E_γ . The experimental data are from Ref. ¹⁶ and the solid lines are from the calculation of Ref. ¹⁷.

we use the SAID program for the pion photoproduction amplitudes. Actually there is no experimental data for the total cross sections for pion photoproduction and the data shown in Fig. 3 are *not* experimental data but are extracted from the SAID program based on Ref. ¹⁷. There can be a few comments on this method. First, the SAID program is established to be valid up to $E_\gamma = 2$ GeV and the extrapolation to the higher energy cannot be guaranteed. Therefore we will use the program only in the limited energy region $W \leq 2$ GeV. Second, the SAID program is believed to represent the experimental data. This means that the extracted amplitude should be assumed to include all nucleon resonance effects. However, since there is no simple meson-exchange model for pion photoproduction within our energy region, we will use this amplitude keeping its limitation in mind. The comparison of the model and the data are given in Fig. 5.

We next need the amplitude for pion induced ω production. This reaction has been discussed in Refs. ^{24,25,26,27} recently. It was also recently claimed that the final state interactions including nucleon resonances are very crucial to explain the experimental data in Ref. ²⁷. Following Refs. ^{26,27}, in this study we use the model shown in Fig. 6 concentrating on the low energy

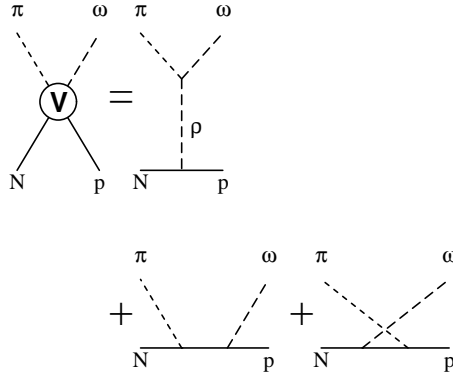


Figure 6. A model for $\pi N \rightarrow \omega p$ reaction.

region, which is consistent with those model studies. In addition to the $\omega\rho\pi$ interaction Lagrangian (5), we need the ωNN and the ρNN couplings. As in our previous studies³, we use

$$g_{\omega NN} = 10.35, \quad \kappa_{\omega} = 0, \quad g_{\rho NN} = 6.12, \quad \kappa_{\rho} = 3.1, \quad (7)$$

where the ρ -nucleon coupling is consistent with the ρ coupling universality. Then the scattering amplitude includes the isospin factor, which reads

$$C_I = \begin{cases} +1 & \text{for } \pi^0 p \rightarrow \omega p \\ \sqrt{2} & \text{for } \pi^- p \rightarrow \omega n, \pi^+ n \rightarrow \omega p \\ -1 & \text{for } \pi^0 n \rightarrow \omega n \end{cases} \quad (8)$$

The form factors of the vertices can be found, for example, in Ref.²⁶. The calculated total cross section for $\pi^- p \rightarrow \omega n$ is shown in Fig. 7.^a

3 Results and Discussions

With the amplitudes discussed so far, we first compute the differential cross section for ω photoproduction at $E_{\gamma} = 1.23$ GeV and 1.68 GeV. The preliminary results are shown in Fig. 8. Since the purpose of this calculation is a rough estimate on the role of the final state interactions, we do not try to adjust parameters to fit the experimental data in this calculation. In Fig. 8,

^a The experimental data for the cross section of this reaction near threshold is controversial^{27,28}. In Fig. 7 we follow Ref.²⁷.

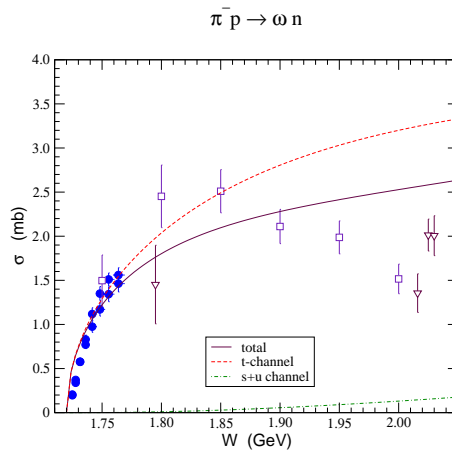


Figure 7. Total cross section for $\pi^- p \rightarrow \omega n$.

the solid lines are the results at tree level³, the dotted lines are from the intermediate $\rho^0 p$ state. The intermediate $\pi^0 p$ and $\pi^+ n$ channels are represented by dashed and dot-dashed lines, respectively.

As we expected from Fig. 3 the contributions from these channels are not suppressed compared to the tree level results. Especially the charged pion channel gives the most important contribution among the intermediate state considered here. The role of the neutral pion intermediate state seems to be smaller than the other channels in the considered energy region. Since the ω photoproduction cross section is at the same order magnitude as the neutral pion photoproduction cross section and smaller than the ρ photoproduction cross section, the contribution from the intermediate ωp channel is expected to be smaller than that from the ρp channel.

We also note that the differential cross section from the intermediate pion channel strongly depends on the momentum transfer t . While the ρp channel differential cross sections do not strongly depend on the scattering angle θ , the pion channel contribution gives rise to strong peaks at backward angles like the u -channel nucleon exchange. Thus, careful analyses are required to distinguish the two mechanisms at backward scattering angles.

In summary, we calculate the one loop contribution to ω photoproduction with selected intermediate states. We found that the final state interactions, especially charged pion intermediate state, are not negligible in the considered energy region and may affect the parameters of the nucleon resonances which

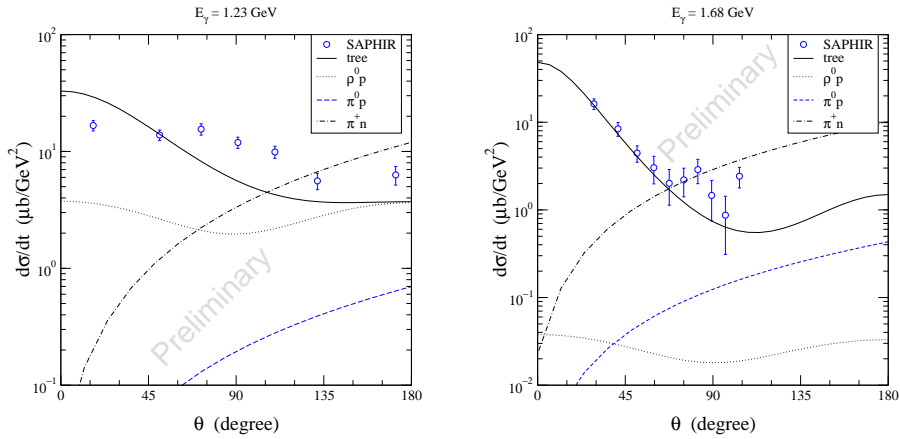


Figure 8. Differential cross sections for $\gamma p \rightarrow \omega p$ at $E_\gamma = 1.23$ GeV (left panel) and 1.68 GeV (right panel). θ is the scattering angle in the center-of-mass frame. The experimental data are from SAPHIR ²⁹.

will be extracted from the forthcoming experimental data. Since the polarization asymmetries are suggested to be the most useful tools to investigate nucleon resonances, it would also be important to check the contribution from the final state interactions to the polarization asymmetries.

Acknowledgments

Y.O. is grateful to Prof. M. Fujiwara for the warm hospitality during the symposium. This work was supported in part by the Brain Korea 21 project of Korean Ministry of Education, the International Collaboration Program of KOSEF under Grant No. 20006-111-01-2, and U.S. DOE Nuclear Physics Division Contract No. W-31-109-ENG-38.

References

1. S. Capstick and W. Roberts, JLAB Report (2000), nucl-th/0008028.
2. Q. Zhao, Z. Li, and C. Bennhold, Phys. Rev. C **58**, 2393 (1998).
3. Y. Oh, A. I. Titov, and T.-S. H. Lee, Phys. Rev. C **63**, 025201 (2001); Talk at SPIN 2000 Symposium (2000), nucl-th/0012012; Talk at NSTAR 2001 Workshop (2001), nucl-th/0104046.
4. Q. Zhao, Phys. Rev. C **63**, 025203 (2001); these proceedings.

5. A. I. Titov and T.-S. H. Lee, these proceedings.
6. Y. Oh, A. I. Titov, and T.-S. H. Lee, Talk at NSTAR 2000 Workshop (2000), nucl-th/0004055.
7. S. Nozawa, B. Blankleider, and T.-S. H. Lee, Nucl. Phys. A **513**, 459 (1990).
8. T. Sato and T.-S. H. Lee, Phys. Rev. C **54**, 2660 (1996).
9. A. Donnachie and P. V. Landshoff, Nucl. Phys. B **244**, 322 (1984); **B267**, 690 (1986); Phys. Lett. B **185**, 403 (1987); **296**, 227 (1992).
10. M. Froissart, Phys. Rev. **123**, 1053 (1961).
11. A. Martin, Phys. Rev. **129**, 1432 (1963).
12. U. Maor and P. C. M. Yock, Phys. Rev. **148**, 1542 (1966).
13. K. Schilling and F. Storim, Nucl. Phys. B **7**, 559 (1968).
14. See, e.g., E. Martynov, E. Predazzi, and A. Prokudin, BITP, Ukraine Report (2001), hep-ph/0112242.
15. C.-T. Hung, S. N. Yang, and T.-S. H. Lee, Phys. Rev. C **64**, 034309 (2001) and references therein.
16. The Durham RAL Databases, <http://durpdg.dur.ac.uk/HEPDATA/REAC>.
17. D. Dutta, H. Gao, and T.-S. H. Lee, MIT Report (2001), nucl-th/0111005.
18. B. Friman and M. Soyeur, Nucl. Phys. A **600**, 477 (1996).
19. F. Klingl, N. Kaiser, and W. Weise, Z. Phys. A **356**, 193 (1996).
20. Ö. Kaymakçalan, S. Rajeev, and J. Schechter, Phys. Rev. D **30**, 594 (1984).
21. P. Jain, R. Johnson, U.-G. Meissner, N. W. Park, and J. Schechter, Phys. Rev. D **37**, 3252 (1988).
22. F. Kleefeld, E. van Beveren, and G. Rupp, Nucl. Phys. A **694**, 470 (2001).
23. T. Fujiwara, T. Kugo, H. Terao, S. Uehara, and K. Yamawaki, Prog. Theor. Phys. **73**, 926 (1985).
24. M. Post and U. Mosel, Nucl. Phys. A **688**, 808 (2001).
25. M. Lutz, G. Wolf, and B. Friman, Nucl. Phys. A **661**, 526c (1999).
26. A. I. Titov, B. Kämpfer, and B. L. Reznik, FZ Rossendorf Report (2001), nucl-th/0102032.
27. G. Penner and U. Mosel, Universität Giessen Report (2001), nucl-th/0111023; nucl-th/0111024.
28. C. Hanhart and A. Kudryavtsev, Eur. Phys. J. A **6**, 325 (1999).
29. F. J. Klein, Ph.D. thesis, Bonn University (1996); π N Newslett. **14**, 141 (1998).